

CAL-B catalyzed desymmetrization of 3-alkylglutarate: "olefin effect" and asymmetric synthesis of pregabalin†

Cite this: DOI: 10.1039/c3ob40311d

Jae-Hoon Jung,^a Doo-Ha Yoon,^a Philjun Kang,^b Won Koo Lee,^{*b} Heesung Eum^a and Hyun-Joon Ha^{*a}

CAL-B catalyzed desymmetrization of prochiral 3-alkylglutaric acid diesters was performed to prepare optically active 3-alkylglutaric acid monoesters bearing various alkyl substituents, including methyl, ethyl, propyl and allyl groups. Allyl esters showed far better stereoselectivity among the alkyl esters, suggesting possible π - π interactions between the olefin of the substrate and the Trp104 or His224 side chains at the enzyme active site. Based on this reaction, the synthesis of (S)-(+)-3-aminomethyl-5-methylhexanoic acid (pregabalin) was achieved with a 70% overall yield.

Received 12th February 2013,
Accepted 28th February 2013

DOI: 10.1039/c3ob40311d

www.rsc.org/obc

Introduction

Obtaining an optically pure isomer that is free from other stereoisomers is strongly demanded, particularly in the pharmaceutical industry,¹ which drives the development of various catalysts including enzymes. Among many industrially applicable enzymes, lipases are the most useful to catalyze diverse reactions based on the carbonyl functionality of carboxylic acids and their derivatives.² Many different types of lipases are available from various sources including mammalian cells and diverse microorganisms. Furthermore, most lipases are tolerant of a wide spectrum of substrates and reaction media. However, there is a significant limitation in obtaining optically pure compounds from lipase-mediated resolution of racemates, and only 50% reaction yields can be obtained. To overcome this limitation, racemization of the unreacted isomer with a strong base or a metal complex is a possible alternative.³ Desymmetrization is another way to produce an optically pure reaction product with a 100% theoretical yield in the absence of a racemizer.⁴ Various chemical and enzymatic methods have been reported for desymmetrization to yield optically pure products. However, few studies have reported the chemical and enzymatic desymmetrization of 3-alkylglutaric acid diesters to obtain chiral 3-alkylglutaric acid monoesters, which are good starting materials for biologically important molecules.⁵ One of the representative examples is

3-((alkyloxycarbonyl)methyl)-5-methylhexanoic acid, which is a synthetic precursor for pregabalin[®],⁶ a lipophilic GABA (γ -aminobutyric acid) analogue for treating several central nervous system disorders including epilepsy, neuropathic pain, anxiety and social phobia.⁷ Though there is a success story⁵ of desymmetrization of diisopropyl 3-isobutylglutarate by porcine liver esterase with 70% ee a more stereoselective method is still needed. In this study, enzymatic desymmetrization of 3-alkylglutaric acid diesters was undertaken to achieve a practical synthetic route to prepare pregabalin. We describe one of the most efficient synthetic routes for pregabalin through lipase-mediated desymmetrization of 3-alkylglutaric acid diesters. In addition, a systematic study of the enzymatic desymmetrization of the 3-alkylglutaric acid diesters provides valuable information regarding the active site binding mode, which is dependent not only on the alkyl group at C3 but also the alkyl group at the ester. Many structurally diverse organic molecules have been utilized as lipase substrates for reactions, including hydrolysis, esterification and ammoniolysis, some of which provide quite clear pictures of the binding mode near the active site residues combined with their crystalline structures.² However, there are still many uncertainties predicting the reactivity and stereoselectivity of certain substrates due to enzyme mobility and remote interactions. Throughout this study, we found an "olefin effect", in which the diallyl esters among other alkyl esters showed far better stereoselectivity with possible remote interactions between the substrate and the enzyme active site.

CAL-B catalyzed desymmetrization of 3-alkylglutarates

The first step focused on enzymatic desymmetrization of prochiral 3-isobutylglutaric acid, its diesters, and anhydrides with

^aDepartment of Chemistry and Protein Research Center for Bio-Industry, Hankuk University of Foreign Studies, Yongin, Kyunggi-Do 449-719, Korea. E-mail: hjha@hufs.ac.kr; Tel: +82-31-330-4369

^bDepartment of Chemistry, Sogang University, Seoul 121-742, Korea. E-mail: wonkoo@sogang.ac.kr; Tel: +82-2-705-8449

†Electronic supplementary information (ESI) available: Preparation of substrates. NMR spectra. HPLC data for ee values. Further results of molecular dynamics simulation. See DOI: 10.1039/c3ob40311d

some commercial lipases including CAL-B (an immobilized lipase B from *Candida antarctica*), porcine pancreatic, *Pseudomonas cepacia*, *Candida cylindracea*, *Aspergillus niger*, *Rhizopus niveus*, *Rhizopus arrhizus*, wheat germ, and porcine liver esterase. Enzymatic desymmetrization of 3-isobutylglutaric acid and its anhydride with alcohols in toluene did not yield the corresponding monoester products over 24 hours. Thus, we switched our attention to the selective hydrolysis of prochiral dialkyl 3-isobutylglutarate prepared from esterification of the corresponding diacids. Fortunately, two enzymes, CAL-B and porcine liver esterase, were active in the hydrolytic reaction of diethyl 3-isobutylglutarate (**1b**), and CAL-B was slightly better than porcine liver esterase. We thereby decided to further study the CAL-B enzyme to determine how efficiently the desymmetrization proceeds and how good the stereoselectivity would be by changing the alkyl group of prochiral dialkyl 3-isobutylglutarate (**1**).

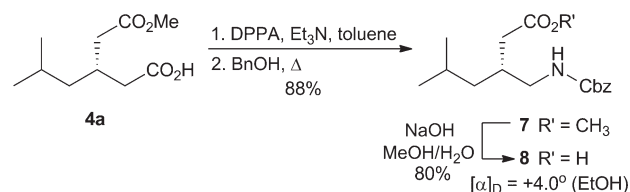
The typical reaction was carried out with the enzyme in phosphate buffer at pH 7 with a pH adjustment throughout the reaction using 0.25 M NaOH (Table 1). After completion of the hydrolytic reaction in 5.1 h, the reaction product, a monoethyl ester of 3-isobutylglutaric acid (**4b**), was obtained at a quantitative yield of 76% enantiomeric excess (ee) (entry 2).

Prochiral dimethyl (**1a**) and dipropyl 3-isobutylglutarates (**1c**) were prepared and reacted with CAL-B to obtain their corresponding monoesters (**4a** and **4c**) in quantitative yields (entries 1 and 3). As expected, the stereochemical outcomes were also quite similar to the ethyl case with 75 and 50% ee, respectively.

The diallyl esters (**1d**) showed astonishingly improved stereoselectivity of 93% ee without sacrificing the reaction yield, which was the average of quadruplicates with different reaction scales from several hundred milligrams up to several grams (entry 4). However, the di-*i*-butyl ester (**1e**) substrate, bearing one additional carbon chain on the allyl or propyl group, was quite inert to the hydrolytic reaction after 36 hours (entry 5). The difference in the ee between the propyl and allyl esters at 50 and 93% was equivalent to 1.197 kcal mol⁻¹ to

discriminate one enantiomer from the other by the specific interactions between the substrates and the enzyme. Propyl and allyl groups have the same carbon-chain length, but the allyl group has olefin at the end rather than a saturated alkane seen in the propyl group. This “olefin effect” was further investigated with 3-propyl (**2**) and 3-methylglutarates (**3**). Dipropyl (**2c**) and diallyl (**2d**) 3-propylglutarates were reacted with the CAL-B enzyme under all of the same conditions. A larger difference in stereoselectivity was observed in the dipropyl (**2c**) and diallyl (**2d**) 3-propylglutarates, with ee values of 12 and 72%, respectively (entries 6 and 7). The chemically similar esters such as dipropargyl (**2e**) and dicyclopropylmethyl (**2f**) 3-propylglutarates showed poor stereoselectivities of 35 and 15% ee compared to those of allylesters (**2d**) (entries 8 and 9). These results highlight the “olefin effect” that was not observed either in the alkynyl group with two π -bonds or in the conformationally less mobile cyclopropylmethyl group. Hydrolytic reactions of dipropyl (**3c**) and diallyl (**3d**) 3-methylglutarates revealed ee values of 11 and 15% which were quite poor, but there was still some “olefin effect” (entries 10 and 11).

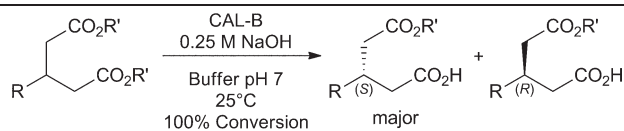
To determine the absolute stereochemistry of the hydrolyzed **4a**, the carboxylic acid was converted to the Cbz-protected amine **7** followed by hydrolysis to yield amino acid **8**. The $[\alpha]_D^{25}$ value was +4.0°, indicating that the absolute stereochemistry of the amino acid was 3*R*.⁸ Therefore, the desymmetrization reaction of prochiral dialkyl 3-isobutylglutarates proceeded to give the monoester as a product with a 3*S* configuration (Scheme 1).



Scheme 1 Stereochemical identification of the 3-isobutylglutaric acid monoester hydrolytic product (**4a**).

Table 1 CAL-B catalyzed desymmetrization of prochiral dialkyl 3-isobutylglutarate (**1–3**)

Entry	S.M.	R	R'	Conversion (%)	Reaction time (h)	Product (ee)
1	1a	<i>i</i> -Bu	Me	100	5.0	4a (75)
2	1b	<i>i</i> -Bu	Et	100	5.1	4b (76)
3	1c	<i>i</i> -Bu	Pr	100	15.5	4c (50)
4	1d	<i>i</i> -Bu	Allyl	100	15.6	4d (93)
5	1e	<i>i</i> -Bu	<i>i</i> -Bu	5	36.0	—
6	2c	Pr	Pr	100	12.7	5c (12)
7	2d	Pr	Allyl	100	5.7	5d (72)
8	2e	Pr	Propargyl	100	1.4	5e (35)
9	2f	Pr	Cyclopropylmethyl	100	3.0	5f (15)
10	3c	Me	Pr	100	0.4	6c (11)
11	3d	Me	Allyl	100	0.2	6d (15)



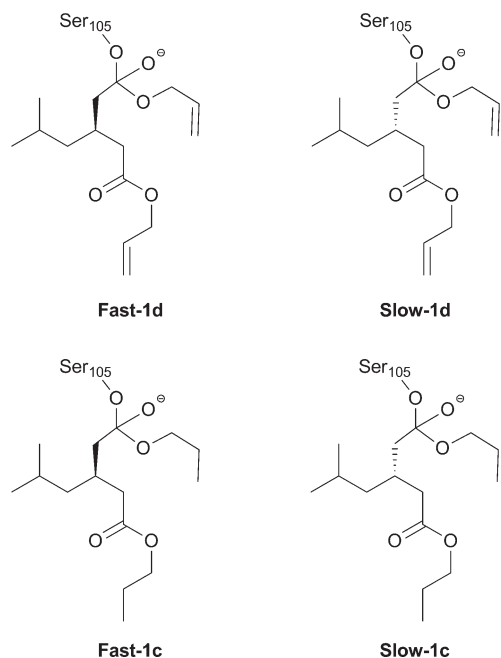


Fig. 1 Tetrahedral intermediates (T_{d1}) of the selected substrates with different configurations during individual 15 ns molecular dynamics simulations.

Molecular dynamics study

Then, we determined the role of this olefin by directly comparing the diallyl and dipropyl 3-isobutylglutarate during binding at the active site of the CAL-B enzyme with a 15 ns molecular dynamics (MD) simulation based on the first tetrahedral intermediate T_{d1} for serine esterase-catalyzed hydrolysis. Four different tetrahedral intermediates (T_{d1}) of the selected substrates were generated with different configurations such as **Fast-1d**, **Slow-1d**, **Fast-1c**, and **Slow-1d** (Fig. 1).

The tetrahedral intermediate T_{d1} must form six catalytically essential hydrogen bonds (D1–D6), containing three for the oxyanion hole (D1–D3) and another three for the catalytic triad (D4–D6) with lipase, as shown in Fig. 2 with the representative substrate **1d**.

The formation and collapse of the tetrahedral intermediate T_{d1} dominated the enzymatic reaction suggesting that T_{d1} resembled the transition state of the catalytic reaction.⁹ Therefore, the origin of the kinetic resolution by lipase-catalyzed hydrolysis should be studied by inspecting T_{d1} through MD simulations. The six essential hydrogen bond interactions between the substrate and the active site in the tetrahedral intermediate T_{d1} were investigated for each of four substrates (**Fast-1d**, **Slow-1d**, **Fast-1c** and **Slow-1c**). They were evaluated by comparison with known criteria^{10,11} including the atomic distance (N–O or O–O < 3.1 Å)¹² and the bond angle (N–H–O or O–H–O > 120°) (Fig. 2). All essential hydrogen bonds (D1–D6) generated from the four different substrates were sufficiently effective to proceed without a notable difference to explain the selectivity observed in the allyl ester.

Further investigation into the transition state featured new descriptors including the non-bonding interaction distances

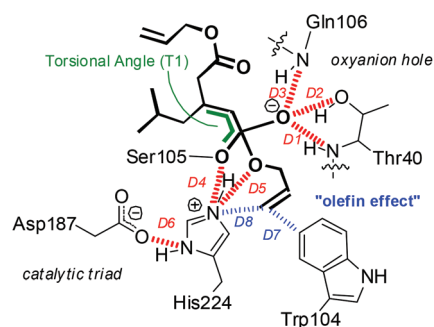


Fig. 2 The tetrahedral intermediate T_{d1} shows the schematic details of active site residues including Trp104 where the allyl group binds. Active site details feature the hydrogen bonds essential for catalysis (red dotted lines D1–D6) and the distances from the olefinic carbon at the substrate to the nearest aryl carbon in the Trp104 side chain (D7) and to the nearest N3 of the imidazole ring attached at the catalytic His224 (D8).

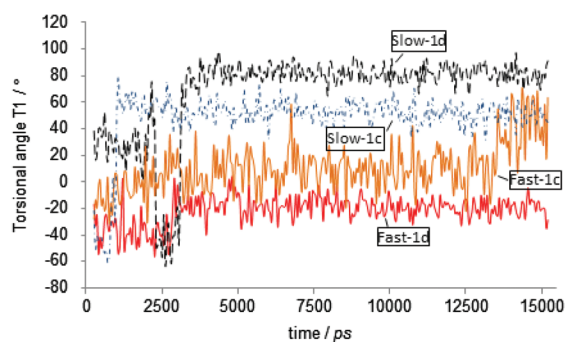


Fig. 3 Results of the molecular dynamics simulation between the fast and slow-reacting substrates (**Fast-1d** vs. **Slow-1d** and **Fast-1c** vs. **Slow-1c**) based on the difference in the T1 torsional angle.

(D7 and D8) and the T1 torsional angle around the active carbonyl group (Fig. 2). The D7 descriptor represents the distance between the olefinic carbon in the substrate and the nearest aryl carbon in the Trp104 side chain which is positioned at the nearby active site. Another descriptor D8 shows the distance between the olefinic carbon in the substrate and the nearest N3 of the imidazole ring attached at the catalytic His224. We observed that the more selective substrates (**1d** vs. **1c**) showed a larger difference in the T1 torsional angle, *i.e.* the torsional angle difference between **Fast-1d** and **Slow-1d** was much bigger than the same angle difference between **Fast-1c** and **Slow-1c**.

Moreover, the T1s torsional angles for **Slow-1d**, **Fast-1c** and **Slow-1c** gradually approached about 60° of unreactive geometry, whereas only **Fast-1d** went to 0° as a favorable conformer (Fig. 3).¹⁰

The results of the MD study for the descriptors D7 and D8 showed the π - π interactions between the olefin of the substrate and the Trp104 and His224 side chain at the active site (Fig. 4 and Table 2). The average distance D7 for the **Fast-1d** between the olefin in the substrate and the aryl group in Trp104 was 4.20 Å, which was shorter than that of the **Slow-1d** substrate at 4.63 Å. A similar difference was observed for the **Fast-1d** and

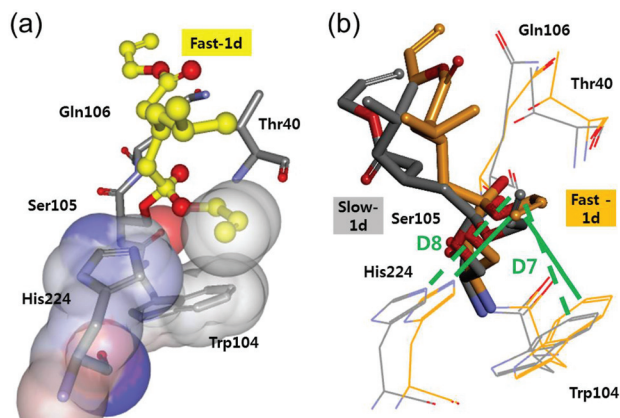


Fig. 4 (a) The three-dimensional T_d1 structure of **Fast-1d** at the enzyme active site. Three different functional groups including the olefin in the substrate, His224 and Trp104 at the active site were close together and expressed by the surface filling model. (b) A comparison of the three-dimensional T_d1 structure of **Fast-1d** (brown colored molecule) vs. **Slow-1d** (grey colored molecule) at the active sites. Green solid lines show the strong interactions among three nearby groups including the olefin in the substrate and His224 and Trp104 at the active site of **Fast-1d**. Green dotted lines show the same but weak interactions of **Slow-1d**.

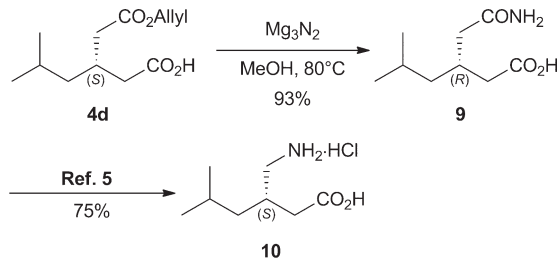
Table 2 **Fast-1d** and **Slow-1d** distances D7 and D8 generated from the molecular dynamics simulation snapshots

	D7		D8	
	Fast-1d	Slow-1d	Fast-1d	Slow-1d
Average (Å)	4.20	4.63	3.94	4.24
Total snapshots (15 ns)	300	300	300	300
Within criteria ^a	122	21	207	99
% ^a	41	7	69	33

^a Distance criteria were less than 4.0 Å between the olefinic carbon in the substrate and the nearest aryl carbon in the side chain of Trp104 (D7) and the nearest N3 of the imidazole ring attached at the catalytic His224 (D8).

Slow-1d substrates in D8 (3.94 and 4.24 Å, respectively), which was the distance between the olefin in the substrate and the nearest N3 of the imidazole ring attached at the catalytic His224. The effective distances D7 and D8 for the nonbonding interaction were less than 4.0 Å,¹³ and a large difference was observed in the snapshots of each enantiomer during the 15 ns. Among 300 cases, 122 (41% for D7) and 207 (69% for D8) snapshots were effective for **Fast-1d**, compared to only 21 (7% for D7) and 99 (33% for D8) snapshots for **Slow-1d**. The olefin in the case of **Fast-1d** drove the favorable conformation change in T_d1 with a big discrimination against **Slow-1d**, which we called the “olefin effect”.¹⁴

Undoubtedly, the experimental and modeling results corroborate the “olefin effect” between the substrate and the enzyme,¹⁵ which was the crucial factor increasing the enantioselectivity on the CAL-B catalyzed desymmetrization of prochiral 3-alkylglutaric acid diallylesters over other esters.



Scheme 2 Pregabalin synthesis.

Pregabalin synthesis

The hydrolytic reaction product was utilized to prepare (*S*)-(+)-3-aminomethyl-5-methylhexanoic acid (**10**) (pregabalin). Conversion of the ester (**4d**) to an amide (**9**) was achieved in a highly efficient manner without racemization and no interference of carboxylic acid with Mg_3N_2 in methanol.¹⁶ Amide **9** was recrystallized twice in diethyl ether to produce an enantiomerically pure product in 93% yield. This was the synthetic precursor used for preparing pregabalin,⁵ which is administered to treat several diseases related to the central nervous system (Scheme 2).⁷

Conclusions

In conclusion, we examined the “olefin effect” on the CAL-B catalyzed-hydrolytic reaction of prochiral diallyl 3-alkylglutarate. We also successfully synthesized pregabalin from the hydrolytic product 3-((allyloxy-carbonyl)methyl)-5-methylhexanoic acid (**4d**) through two consecutive steps including transformation of the ester to the corresponding amide and a Hoffman rearrangement with a 70% overall yield.

Experimental

The CAL-B, CHIRALZYME® L-2, c.-f., lyo, was purchased from Roche. The high performance liquid chromatography (HPLC) analysis was performed using a YL 9100 HPLC system with a UV/VIS detector. ¹H NMR and ¹³C NMR spectra were obtained using a Varian 200 (200 MHz for ¹H and 50.3 MHz for ¹³C) spectrometer and deuterated solvents ($CDCl_3$ + 0.03% TMS, CD_3OD ; Euriso-top®). Optical rotation was measured using a polarimeter (Rudolph Autopol IV digital polarimeter). Low and high resolution mass spectrometry (MS) analyses were performed using a Macromass ZQ4000 LC/MS system and an AB Sciex 4800 Plus MALDI TOF/TOF™ with a 2,5-dihydroxybenzoic acid (DHB) matrix was used to prepare samples for MS. Data were obtained in the reflector positive mode with internal standards for calibration, respectively.

Analytical methods

After CAL-B-mediated hydrolysis, a chiral HPLC method was used to analyze the mono-ester products obtained. The mono-

ester products **4a–6d** were analyzed with a Chiralpak® IA (4.6 mm × 250 mm) using IPA–hexane–TFA 1 : 99 : 0.1, 0.3 mL min⁻¹ (**5c**) or 0.7 mL min⁻¹ (**5d**), IPA–hexane 2 : 98, 0.6 mL min⁻¹ (**6c–6d**) and **4a–4e**, **5e–5f** were analyzed by Chiralcel® OD-RH (4.6 mm × 150 mm) using IPA–ACN–TFA 97 : 3 : 0.1, 0.4 mL min⁻¹, H₂O–ACN 80 : 20, 0.3–0.8 mL min⁻¹ and detection at 210–215 nm.

General procedure for CAL-B mediated hydrolysis

Dialkyl 3-alkylpentanedioate (0.65 mmol) was diluted in phosphate buffer solution (pH 7) at 25 °C. When the pH had stabilized, CAL-B (180 mg) was added to the solution. pH was maintained with NaOH (0.25 M, 2.6 mL, 0.65 mmol). The reaction mixture was diluted with EtOAc (10 mL) and filtered. The aqueous layer was extracted with EtOAc (2 × 20 mL). The organic layer extracts were dried over MgSO₄, filtered, and concentrated *in vacuo*. The % ee value of the given compound as a yellow oil (99%) was measured using the chiral HPLC method.

(R)-Methyl 3-((benzyloxycarbonylamino)methyl)-5-methylhexanoate 7

TEA (0.072 mL, 0.52 mmol, 1 equiv.) and DPPA (0.11 mL, 0.52 mmol, 1 equiv.) were added to a solution of (*S*)-3-(2-methoxy-2-oxoethyl)-5-methylhexanoic acid **4a** (104.3 mg, 0.52 mmol, 1 equiv.) in toluene (1.3 mL) at room temperature. The solution was warmed to 90 °C and stirred for 2 h. Benzyl alcohol (0.053 mL, 0.52 mmol, 1 equiv.) was added, and the reaction mixture was refluxed overnight. The reaction mixture was washed with a solution of 1% NaNO₂ and 1.5% NaHCO₃ in H₂O (2 × 100 mL), followed by H₂O (100 mL). The organic layer was dried over MgSO₄, filtered, and concentrated *in vacuo*. The crude compound was purified by column chromatography on silica gel (9 : 1 Hex–EtOAc) to furnish the *title compound* **7** (141 mg, 88%) as a colorless oil. [α]_D²⁵ +3.84° (c1.51, EtOH); ¹H NMR (200 MHz, CDCl₃): δ = 0.89 (m, 6H), 1.10–1.25 (m, 2H), 1.58–1.64 (m, 1H), 2.13–2.31 (m, 3H), 3.08–3.32 (m, 2H), 3.65 (s, 3H), 4.93 (s, 1H), 5.10 (s, 2H), 7.35 (m, 5H); ¹³C NMR (50 MHz, CD₃OD): δ = 171.78, 155.64, 135.05, 126.05, 125.54, 125.39, 63.98, 48.59, 42.14, 39.22, 34.71, 31.62, 22.97, 19.69; HRMS–MALDI (*m/z*): [M + Na]⁺ calcd for C₁₇H₂₅NaNO₄, 330.1676; found, 330.1674.

(R)-3-((Benzyloxycarbonylamino)methyl)-5-methylhexanoic acid 8

NaOH (25 mg, 0.63 mmol, 2 equiv.) was added to a solution of (*R*)-methyl 3-((benzyloxycarbonylamino)methyl)-5-methylhexanoate **7** (97 mg, 0.32 mmol, 1 equiv.) in MeOH–H₂O (8 : 1, 2 mL) at room temperature. The reaction mixture was stirred for 4 h, and then MeOH was evaporated *in vacuo*. The reaction mixture in H₂O was acidified with 3 N HCl to pH 3–4, and extracted with DCM (3 × 30 mL). The organic layer was dried over MgSO₄, filtered and concentrated *in vacuo*. The crude compound was purified by column chromatography on silica gel (1 : 1 Hex–EtOAc) to furnish *title compound* **8** (74 mg, 80%) as a yellow oil. [α]_D²⁵ +4.00° (c1.20, EtOH); ¹H NMR (200 MHz, CDCl₃): δ = 0.89 (m, 6H), 1.13–1.33 (m, 2H), 1.60–1.66 (m, 1H),

2.05–2.37 (m, 3H), 3.07–3.34 (m, 2H), 5.03 (s, 1H), 5.10 (s, 2H), 7.35 (m, 5H); ¹³C NMR (50 MHz, CD₃OD): δ = 176.83, 159.08, 138.45, 129.42, 128.90, 128.71, 67.37, 45.47, 42.56, 38.28, 34.95, 26.34, 23.05; HRMS–MALDI (*m/z*): [M + Na]⁺ calcd for C₁₆H₂₃NaNO₄, 316.1519; found, 316.1524.

(R)-3-(2-Amino-2-oxoethyl)-5-methylhexanoic acid 9

Mg₃N₂ (0.155 g, 1.53 mmol, 5 equiv.) was added to a solution of (*S*)-3-(2-(allyloxy)-2-oxoethyl)-5-methylhexanoic acid **4d** (70.1 mg, 0.31 mmol, 1 equiv.) in MeOH (1.3 mL) at room temperature. The mixture was warmed to 80 °C and stirred for 16 h. The reaction mixture was acidified to pH 3–4 with 6 N HCl. The aqueous layer was extracted with EtOAc (3 × 30 mL). The organic layer was dried over MgSO₄, filtered, and concentrated *in vacuo*. The crude compound was purified by recrystallization in Et₂O (20 mL) to furnish *title compound* **9** (53.9 mg, 93%) as a white solid. ¹H NMR (200 MHz, DMSO-*d*₆): δ = 0.80 (d, *J* = 6.4 Hz, 6H), 1.07 (t, *J* = 6.4 Hz, 2H), 1.57 (m, 1H), 1.97–2.22 (m, 5H), 6.37 (s, 1H), 6.77 (s, 1H); ¹³C NMR (50 MHz, DMSO-*d*₆): δ = 174.7, 174.6, 43.8, 40.4, 30.4, 25.2, 23.3, 23.3; MS (*m/z*): [M + Na]⁺ calcd for C₉H₁₇NO₃Na, 210.11; found, 209.88; Mp 131–135 °C.

Molecular modeling

Preparation of the MD simulation

Proteins were prepared using Discovery Studio 2.5 (Accelrys Inc., San Diego, CA, USA). The starting crystal structure of CAL-B (PDB ID: 1TCA) was taken from the Protein Data Bank.¹⁷ All simulations were performed using the CHARMM force-field.¹⁸ The missing atoms and residues in the structure were added at pH 7.0. The partial charges of the tetrahedral intermediate were set according to the Momany–Rone calculation in this and subsequent steps.¹⁹ This includes three stages of minimization: (1) minimization of just hydrogen atoms while all heavy atoms are fixed; (2) minimization of all hydrogens and side chain atoms while all backbone atoms are fixed and (3) minimization of all atoms. The water molecules from the X-ray structure and hydrogen in the Ser105O γ side chain were removed, and Ser105O γ was covalently bound to the tetrahedral hemiacetal carbon and the catalytic His224 residue was protonated. The first gentle minimization of enzyme was briefly performed with the Smart Minimizer algorithm composed of the steepest descent and conjugate gradient with 5000 steps set to 0.001 kcal mol⁻¹ Å of RMS gradient during generalized Born solvation. Next, **Fast-1d**, one of the fast-reacting substrates as a reference ligand, was covalently bound to Ser105 and the transition state structure (T_{d1}) maintained. Further calculations were carried out for **Slow-1d**, **Fast-1c**, and **Slow-1c**. The ligand was minimized in the same manner by keeping the enzyme fixed. The system was resolved with several water molecules in an explicit spherical boundary with a harmonic restraint set to a 20 Å spherical radius from the mass center to save calculation time.

MD simulation

To minimize all substrates, a standard dynamics cascade was performed by a series of two-stage minimizations, heating, equilibrium, and production by adopting a 12 Å non-bound spherical cut-off, using the isothermal-isochoric ensemble (NVT), and a distance-dependent dielectric implicit solvent model with a dielectric constant set to 1.0. The first minimization was performed with 5000 steps using the steepest descent algorithm with a 0.001 of RMS gradient. The second minimization introduced 50 000 steps with the conjugate gradient and a 0.0001 RMS gradient. Next, the complex was heated with 10 000 steps to a 250 K initial temperature and a 300 K target temperature, and equilibrated with 200 000 steps using a 0.001 time step. Finally, 15 000 000 production stage steps with a 0.001 ps time step yielded the final product generated from 300 snapshots. Only potential or total energy was used to confirm whether the generated conformers were stable or not during MD. All snapshots for each enantiomer were analyzed with focus on the distance and the angle between heteroatoms.

Acknowledgements

This study was supported by the GRRC program of Gyeonggi province (GRRC HUF5-2012-B03) and by the National Research Foundation of Korea (NRF-2011-0012379).

Notes and references

- (a) V. Gotor-Fernández, R. Brieva and V. Gotor, *J. Mol. Catal., B*, 2006, **40**, 111–120; (b) R. N. Patel, *Coord. Chem. Rev.*, 2008, **252**, 659–701; (c) R. N. Patel, *ACS Catal.*, 2011, **1**, 1056–1074; (d) C. M. Clouthier and J. N. Pelletier, *Chem. Soc. Rev.*, 2012, **41**, 1585–1605.
- (a) U. T. Bornscheuer and R. J. Kazlauskas, *Hydrolases in Organic Synthesis: Regio- and Stereoselective Biotransformations*, Wiley-VCH, Weinheim, 2nd edn, 2006, pp. 124–127; (b) K. Faber, *Biotransformations in Organic Chemistry*, Springer, Berlin, 5th edn, 2004, pp. 29–176; (c) V. Gotor, I. Alfonso and E. García-Urdiales, *Asymmetric Organic Synthesis with Enzymes*, Wiley-VCH, Weinheim, 1st edn, 2008, pp. 133–169.
- (a) O. Pàmies and J.-E. Bäckvall, *Chem. Rev.*, 2003, **103**, 3247–3261; (b) B. Martín-Matute and J.-E. Bäckvall, *Curr. Opin. Chem. Biol.*, 2007, **11**, 226–232; (c) J. H. Lee, K. Han, M.-J. Kim and J. Park, *Eur. J. Org. Chem.*, 2010, 999–1015; (d) H. Pellissier, *Tetrahedron*, 2011, **67**, 3769–3802; (e) Y. Kim, J. Park and M.-J. Kim, *ChemCatChem*, 2011, **3**, 271–277.
- Reviews: (a) E. Schoffers, A. Golebiowski and C. R. Johnson, *Tetrahedron*, 1996, **52**, 3769–3826; (b) E. García-Urdiales, I. Alfonso and V. Gotor, *Chem. Rev.*, 2005, **105**, 313–354; Recent examples: (c) N. Ríos-Lombardía, E. Busto, V. Gotor-Fernández and V. Gotor, *J. Org. Chem.*, 2011, **76**, 5709–5718; (d) G. Obame, H. Pellissier, N. Vanthuyne, J. B. Bongui and G. Audran, *Tetrahedron Lett.*, 2011, **52**, 1082–1085; (e) N. Ríos-Lombardía, V. Gotor-Fernández and V. Gotor, *J. Org. Chem.*, 2011, **76**, 811–819; (f) C. Manzuna Sapu, J. E. Bäckvall and J. Deska, *Angew. Chem., Int. Ed.*, 2011, **50**, 9731–9734.
- M. S. Hoekstra, D. M. Sobieray, M. A. Schwindt, T. A. Mulhern, T. M. Grote, B. K. Huckabee, V. S. Hendrickson, L. C. Franklin, E. J. Granger and G. L. Karrick, *Org. Process Res. Dev.*, 1997, **1**, 26–38.
- (a) M. J. Burk, P. D. de Koning, T. M. Grote, M. S. Hoekstra, G. Hoge, R. A. Jennings, W. S. Kissel, T. V. Le, I. C. Lennon, T. A. Mulhern, J. A. Ramsden and R. A. Wade, *J. Org. Chem.*, 2003, **68**, 5731–5734; (b) G. M. Sammis and E. N. Jacobsen, *J. Am. Chem. Soc.*, 2003, **125**, 4442–4443; (c) T. Ok, A. Jeon, J. Lee, J. H. Lim, C. S. Hong and H. S. Lee, *J. Org. Chem.*, 2007, **72**, 7390–7393; (d) C. A. Martinez, S. Hu, Y. Dumond, J. Tao, P. Kelleher and L. Tully, *Org. Process Res. Dev.*, 2008, **12**, 392–398; (e) Y. Chen, X. Li and R. Cheng, *Chin. J. Org. Chem.*, 2011, **31**, 1582–1594; (f) J. M. Liu, X. Wang and Z. M. Ge, *Tetrahedron*, 2011, **67**, 636–640; (g) H. Mukherjee and C. A. Martinez, *ACS Catal.*, 2011, **1**, 1010–1013.
- (a) I. Selak, *Curr. Opin. Invest. Drugs*, 2001, **2**, 828–834; (b) B. A. Lauria-Horner and R. B. Pohl, *Expert Opin. Invest. Drugs*, 2003, **12**, 663–672.
- Z. Hameršak, I. Stipetić and A. Avdagić, *Tetrahedron: Asymmetry*, 2007, **18**, 1481–1485.
- K. Nishizawa, Y. Ohgami, N. Matsuo, H. Kisida and H. Hirohara, *J. Chem. Soc., Perkin Trans. 2*, 1997, 1293–1298.
- (a) J. Nyhlén, B. Martín-Matute, A. G. Sandström, M. Bocola and J.-E. Bäckvall, *ChemBioChem*, 2008, **9**, 1968–1974; (b) J. H. Park, H. J. Ha, W. K. Lee, T. Génereux-Vincent and R. J. Kazlauskas, *ChemBioChem*, 2009, **10**, 2213–2222.
- I. J. Colton, D. L. T. Yin, P. Grochulski and R. J. Kazlauskas, *Adv. Synth. Catal.*, 2011, **353**, 2529–2544.
- M. Cygler, P. Grochulski, R. J. Kazlauskas, J. D. Schrag, F. Bouthillier, B. Rubin, A. N. Serreqi and A. K. Gupta, *J. Am. Chem. Soc.*, 1994, **116**, 3180–3186.
- R. O. Gould, A. M. Gray, P. Taylor and M. D. Walkinshaw, *J. Am. Chem. Soc.*, 1985, **107**, 5921–5927.
- (a) E. A. Meyer, R. K. Castellano and F. Diederich, *Angew. Chem., Int. Ed.*, 2003, **42**, 1210–1250; (b) A. T. Macias and A. D. MacKerell Jr., *J. Comput. Chem.*, 2005, **26**, 1452–1463; (c) L. M. Salonen, M. Ellermann and F. Diederich, *Angew. Chem., Int. Ed.*, 2011, **50**, 4808–4842.
- (a) H. Yang, E. Henke and U. T. Bornscheuer, *J. Org. Chem.*, 1999, **64**, 1709–1712; (b) K. Thodi, E. Barbayianni, I. Fotakopoulou, U. T. Bornscheuer, V. Constantinou-Kokotou, P. Moutevelis-Minakakis and G. Kokotos, *J. Mol. Catal., B*, 2009, **61**, 241–246.
- G. E. Veitch, K. L. Bridgwood and S. V. Ley, *Org. Lett.*, 2008, **10**, 3623–3625.
- J. Uppenburg, M. T. Hansen, S. Patkar and T. A. Jones, *Structure*, 1994, **2**, 293–308.

- 18 A. D. MacKerell Jr, D. Bashford, M. Bellott, R. L. Dunbrack Jr, J. D. Evanseck, M. J. Field, S. Fischer, J. Gao, H. Guo, S. Ha, D. Joseph-McCarthy, L. Kuchnir, K. Kuczera, F. T. K. Lau, C. Mattos, S. Michnick, T. Ngo, D. T. Nguyen, B. Prodhom, W. E. Reiher III, B. Roux, M. Schlenkrich, J. C. Smith, R. Stote, J. Straub, M. Watanabe, J. Wiórkiewicz-Kuczera, D. Yin and M. Karplus, *J. Phys. Chem. B*, 1998, **102**, 3586–3616.
- 19 F. A. Momany and R. Rone, *J. Comput. Chem.*, 1992, **13**, 888–900.